Lightweight and green tiles from recycled polypropylene reinforced with cockle-shells powder

N. Mohamad[1,*], M.A. Zohid, K.I. Karim, M. Mazliah[1], A.R. Jeefferie[1], K.T. Lau[1], R.F. Munawar[1], H.E. Ab Maulod[2]

[1)]Carbon Research Technology, Faculty of Manufacturing Engineering, Universiti Teknikal Malaysia Melaka, Hang Tuah Jaya, 76100 Durian Tunggal, Melaka, Malaysia

[2)]Carbon Research Technology, Faculty of Engineering Technology, Universiti Teknikal Malaysia Melaka, Hang Tuah Jaya, 76100, Durian Tunggal, Melaka, Malaysia

*Corresponding e-mail: noraiham@utem.edu.my

Keywords: Polypropylene: cockle-shells: composite tiles

ABSTRACT – Fabrication of recycled polypropylene filled with cockle-shells composite tiles via melt compounding and hot pressing method were studied. Cockles-shell powder reinforced polypropylene composites were sieved within particle size range of 63µm – 75µm for different weight ratio of 0 wt%, 5 wt%, 10 wt%, 20 wt%, 25 wt% and 30 wt%. Tensile properties was selected as the response. The fracture surface of cockle-hells composite tiles, then were further verified using scanning electron microscopy and fourier transimission infrared radiation. The increasing of cockles-shells powder weight percentage, decrease the tensile strength (14.74MPa to 4.04MPa). In the morphological analysis , limited interaction between fillers and matrices was clearly observed on the fracture surfaces and manifested as voids, cracks, and particles agglomeration also supported by compositional characteristics in term of their their bonding.

1. INTRODUCTION

Polypropylene (PP) is a semi-crystalline thermoplastic that have been used in a varied general application. It is a very versatile and adaptable polymer whereby its properties can readily be enhanced with the inclusion of various types of fillers [1]. It also can possess advantages such a good resistance to fatigue, chemical resistance, excellent moisture resistance, colorfast, transparency, dimensional stability, flame resistance, high heat distortion resistance, high impact strength and a minimal cost polymer type [2]. However, PP is non-degradable due to its chemically stabilized state for long service life; hence the disposal of PP plastic waste causes an environmental issue [3]. Lately, polymer composite is widely used in the production of new engineering materials. In plastic industry, the utilization of inorganic filler in thermoplastic has been a common practice for the dual purposes of reducing production cost of molded products as well as improving the mechanical properties of the thermoplastic. Natural fiber fillers such as cockle-shell have contained of 92-99% by weight of calcium carbonate ($CaCO_3$). Cockle-shell is a form of three main elements such as carbon, oxygen and calcium.

This calcium carbonate is commonly used filler in thermoplastic of composite industry. This due to its minimal cost and can be used at higher percentage load. The presence of calcium carbonate ($CaCO_3$) in composite material can increase the properties of matrix polymer to against deformation, to increase the ductility and impact strength of composites. The combination of polypropylene and cockle-shell powder (CSP) is suitable for the use in the tile industry. In this research, studies on a composite of PP work as matrix and being reinforced by cockle-shells powder for its potential as tile's material will be conducted.

2. METHODOLOGY

Recycled PP from Melaka landfills were washed, cut into smaller pieces and granulated into 'flakes' whereby waste cockle-shell were collected from stall's leftover in Melaka, washed, dried in oven with 100oC for 2 hours, crushed and sieved with average particle size of 69µm. Both of materials then were mixed using the internal mixer via a melt compounding process with 1800C and rotor speed was 60 rpm within 10 minutes. The mixture was prepared with different formulations of (0 wt%, 5 wt%, 10 wt%, 20 wt%, 25 wt% and 30 wt%) of cockle-shell powder reinforced with PP and crushed using crusher machine (GT7013-A, Gotech) at a chosen melting temperature. Pressing process was held at a temperature of 185 0C and pressure of 90 atm with 12 minutes time taken including 2 minutes pre-heating. Then, the obtained sheet was cooled down to room temperature for 4 minutes.

3. RESULT AND DISCUSSION

a. Mechanical properties

Tensile test was conducted based on ASTM D6383535 samples of PP/CS different compositions were cut into 165mm x 19mm x 3mm and shaped into dog-bone sample. The test was carried out by using the Universal Testing Machine with a crosshead speed of 2mm/min. Figure 1 shows the interpreted data of ultimate tensile stress (UTS) with different CSP%. Figure 1 shows the tensile strength drastically decrease from 0 wt% to 10%, become stagnant from 15 wt% to

25 wt% and suddenly drop at 30 wt% of CSP. This might due to the higher crystallinity.

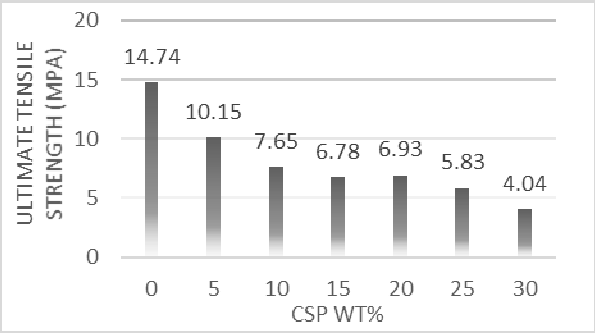

Figure 1 Tensile strength

High tensile strength value at 5 wt% CSP of the composite is due to good filler-matrix interactions, which enable more stress to be transferred from the matrix to the fillers during external loading. For the 30 wt% the tensile strength tends to decrease may due to the uneven distribution of particles in the matrix that lead to the poor bonding. The increase in tensile strength by the addition of filler content be attributed to good interface interaction between filler and matrix, resulting least void and better stress transfer between the filler and matrix [4].

b. Morphological Characteristics

Figure 3 depicts the SEM images for cockle-shells composite tiles after undergone the tensile testing. Figure 2(a) shows higher load of ductility fracture surface of due to the apparent shear yielding mechanism observed. Whereas, the figure 2(b) shows the crack occurred on the 30 wt% CSP due to the lower interaction between PP and CSP. Non-homogeneous distribution resulted in separation between matrix and under loading. This is due to the greater agglomeration of particles compared to 5% to 25% of CSP [5].

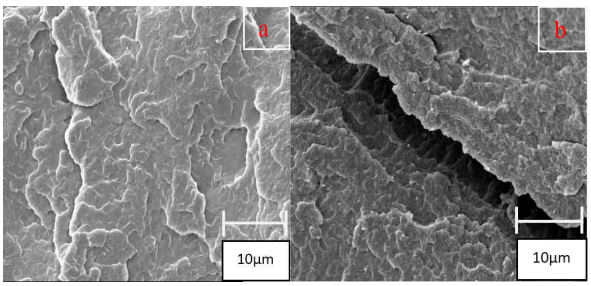

Figure 2 SEM at 500x magnification of: (a) 0 wt% CSP; (b) 30 wt% CSP

c. Compositional characteristics

Figure 3 shows the FTIR spectrum for different composition shows peak pattern of PP added with filler. The bonding stretch between C-H atom might due to the additional of filler into the PP. The wavenumber at 2918 cm^{-1} which indicates the C-H stretch bond of PP in the compound. Furthermore, at the 1733cm^{-1} wavenumber shows the C=O bonding from the $CaCO_3$ while for the peak observed at the 1113cm^{-1} represents C-O due to the breakdown of the $CaCO_3$ from CSP once mixed with the PP.

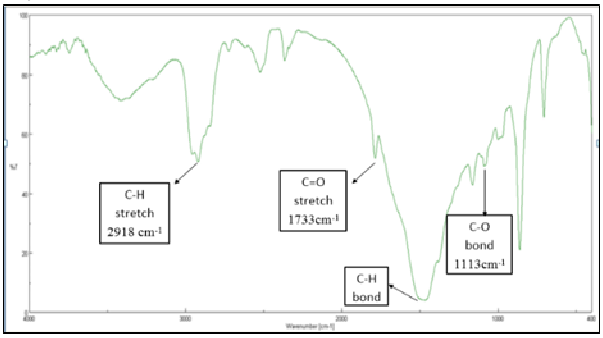

Figure 3 FTIR graph

4. CONCLUSIONS

Recycled PP reinforced with CSP composites tiles are successfully fabricated via melt compounding and hot pressing methods are suitable methods to fabricate. Low amount of CSP to 10 wt% and once CSP was added at 30% were found to decrease the tensile strength. SEM analysis validates the limitation of compatibility between matrix and filler which affected the tensile properties of the composite. Despite the decreasing in tensile strength as expected, however the green tiles have advantages of tiles industry due to the lightweight and cheaper raw materials and production cost.

REFERENCES

[1] M.Y.A. Fuad, H. Hanim, R. Zarina, Z.A. Mohd Ishak, and A. Hassan, "Polypropylene/calcium carbonate nanocomposites – effects of processing techniques and maleated polypropylene compatibiliser," *Express Polymer Letters*, vol. 4, pp. 611-620, 2010.

[2] K. Dey, N. Sharmin, R.A. Khan, S. Nahar, A.J. Parsons and C.D. Rudd, "Effect of Iron Phosphate Glass on the Physico-Mechanical Properties of Jute Fabric-Reinforced Polypropylene-Based Composites," *Journal of Thermo-plastic Composite Materials,* vol. 24, pp. 695-711, 2011.

[3] N. Mohamad, A. Abd Latif, H.E. Ab Maulod, M. A. Azam, M.E. Abd Manaf, "A sustainable polymer composite from recycled polypropylene filled with shrimp shell waste," *Polymer-Plastic Technology and Engineering,* vol. *53,* pp. 167-172, 2014.

[4] P. Kamalbabu and G.C. Mohan Kumar, "Effect of Particle Size on Tensile Properties of Marine Coral Reinforced Polymer Composites," *Procedia Material Science,* vol. 5, pp. 802-808, 2014.

[5] S.O. Adeosun, M.A. Usman, W.A Ayoola, M.A. Bodude, "Physico-Mehcanicals Responses of Polypropylene – $CaCO_3$ Composite," *Minerals and MaterialsCcharacterization and Engineering*, vol. 1, pp. 145-152, 2013.

Gauging user's acceptance of AR mobile application with AR postcards for heritage education in the UNESCO world heritage city of Melaka: Adapting the UTAUT model

L.W. Shang[1,*], T. G. Siang[2], M. H. Zakaria[3]

[1)] Faculty of Information and Communication Technology, Universiti Teknikal Malaysia Melaka, Hang Tuah Jaya, 76100 Durian Tunggal, Melaka, Malaysia
[2)] Faculty of Business, Multimedia University, Jalan Ayer Keroh lama, 75450, Melaka, Malaysia
[3)] Faculty of Information and Communication Technology, Universiti Teknikal Malaysia Melaka, Hang Tuah Jaya, 76100 Durian Tunggal, Melaka, Malaysia

[*]Corresponding e-mail: jaroquelow@hotmail.com

Keywords: User's acceptance; augmented reality; AR postcard; AR mobile application; heritage education

ABSTRACT – Augmented reality (AR) has went through a huge advancement and now AR applications can be executed without issues using modern-day smartphones. This study is aimed towards developing an AR mobile application with AR postcards. Using the application, 3D AR models of historical monuments can be developed which allow tourists to obtain information of the monuments. The application is believed to facilitate a more effective learning experience and appreciation about the history of the heritage monuments. In light of the UTAUT model, this paper envisioned to gauge user's behavioral intention (BI) to use the application based on 50 tourists in Melaka as respondents. Reliability analysis and regression analysis were conducted. PE and FC were found as significant determinants in user's BI the application. Managerial implications for the application developer and policy makers were also discussed.

1. INTRODUCTION

Melaka has been inscribed by the UNESCO as one of the world heritage sites on 7th July 2008. (whc.nesco.org). The prestigious status has made Melaka as one of the most popular tourist attractions in the world with an increasing trend of tourist arrivals and tourism receipts over the years. There has been an increase of number for heritage sites, relics, and objects from around the world that can now be virtually accessible through digitalisation with three-dimensional (3D) models [1]. Past study has discussed about the benefits of digitising the heritage properties into 3D models as 3D models are able to provide and also store extremely precise and accurate data sets through a virtual 3D environment [2]. In regards to these problems, various advancement in digital technologies such as virtual reality (VR) and augmented reality (AR) are now providing practical applications for heritage education. However, the problem with VR is the methods required to operate it. To access VR, a VR head mounted device or a personal computer is needed.

Notably, tourists would not usually possess such bulky devices during their travels. This, however, is not the limitations for AR where various applications can now be accessed using a modern-day smartphone. The modern-day smartphones can facilitate data access and process through a considerable amount of computing power [3]. Through this new method of display which stems from the synergy and capability of modern-day smartphones, content awareness and AR has a great potential to enhance tourists' experience and create exceptional values for them [4]. Therefore, it is possible that mobile AR applications can allow users to explore the environment through adding layers of reality thus resulting in a novel and interactive way of experiencing highly dynamic content [5]. The strengths of the application include being able to introduce AR technology to tourists while sharing information regarding 3D historical monuments and educational information for the tourists. Secondly, mobile AR application solves the problem of space limitation in the real-world scene by providing information in the virtual world. This study aimed to develop the AR mobile application and AR postcard for heritage education in the UNESCO World Heritage City of Melaka. It is strongly believed that the potential of the application can be gauged based on user's acceptance of the application [6]. Thus, this study envisioned to determine user's acceptance of the application by adapting the UTAUT model.

2. METHODOLOGY

The methodology was divided into two main sections, namely: prototype development and pilot testing on user's acceptance of the application.

2.1 Prototype Development

In this study, the standard waterfall model was chosen for the prototype development. The basic AR flows of video capturing, marker tracking, overlaying, and virtual object rendering were successfully applied in the Android OS smartphone. Figure 1 screenshots the outcome of the AR mobile application and AR postcard.

Figure 1 Screenshot of the Prototype

2.2 Test on User's Acceptance of the Application

This study adapted the UTAUT model developed by Venkatesh [7] as the primary theoretical framework, and incorporated an additional determinant, namely playfulness expectancy (PL). Figure 2 illustrates the research framework for this study where Perceived Usefulness (*PU*), Perceived Ease of Use (*PE*), Facilitating Conditions (*FC*), and Perceived Playfulness (PP) were hypothesised as the direct determinants of users' Behavioral Intention to Use (*BI*) the application.

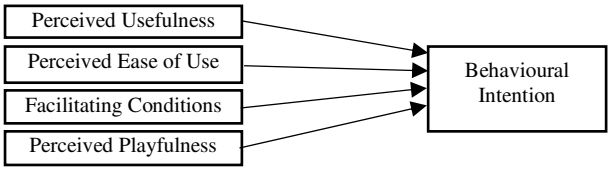

Figure 2 Research Framework

Person-administered survey was conducted using 50 tourists in Melaka as respondents. Data was collected and analyzed using Statistical Package for Social Science (SPSS) version 22.0.

3. RESULT AND DISCUSSION

Firstly, reliability analysis was performed to assess the internal reliability of the measures. All variables scored Cronbach's Alpha statistics of greater than 0.600, namely: *PU* (0.702), *PE* (0.845); *FC* (0.605), *PP* (0.749), and *BI* (0.783). The result reflected a good internal reliability of the data collected [8], which fit for further analyses. Next, regression analysis was performed to examine the relationships among the variables. The Adjusted R Square was 0.512, suggesting that the independent variables explained 51.2% of the total variation in *BI*. Only *PE* and *FC* were found to have a significant ($p < 0.05$) positive relationship with *BI*, with *PE* ($\beta = 0.481$) being the strongest predictor of *BI*, followed by FC ($\beta = 0.371$).

4. CONCLUSION

This study has achieved its objectives as where the AR mobile application with AR postcards were developed for heritage education purpose in the UNESCO World Heritage City of Melaka. The application was successfully implemented into the Android OS platform of smartphones. Also, the pilot testing has been conducted to gauge user's acceptance of the application. The early findings suggested several key implications. The application developer should provide multiple-language content to make the application more user-friendly (*PE*). Also, the policy makers should increase the Wi-Fi hotspots in the UNESCO World Heritage City of Melaka to support the usage of the application (*FC*).

ACKNOWLEDGEMENT

The authors are grateful to the Universiti Teknikal Malaysia Melaka's Zamalah Scheme for the financial sponsorship and continuous support for this study.

REFERENCES

[1] E. Paquet and H.L. Viktor, "Long-term preservation of 3-D cultural heritage data related to architectural sites," in *ISPRS 3D Virtual Reconstruction and Visualization of Complex Architectures*, Mestre-Venice, Italy, August 22-24, 2005.

[2] D.A. Guttentag, Virtual reality: Applications and implications for tourism. Tourism Management, 31(5), 637–651. http://doi.org/10.1016/j.tourman.2009.07.003
Lamport, L. *LaTeX User's Guide and Document Reference Manual.* Addison-Wesley, Reading, MA, 1986.

[3] P. Zheng, and L.M. Ni, *Smart Phone and Next-Generation Mobile Computing*. San Francisco: Morgan Kaufmann Publishers;2006.

[4] Z. Yovcheva, D. Buhalis, and C. Gatzidis, "Overview of smartphone augmented reality applications for tourism", *E-Review of Tourism Research*, 10(2), 63–66, 2012.

[5] C.D. Kounavis, A.E. Kasimati, and E.D. Zamani, "Enhancing the tourism experience through mobile augmented reality: Challenges and prospects", *International Journal of Engineering Business Management*, vol. 4, no. 1, pp. 1–6, 2012.

[6] K. Ab Aziz, and T.G. Siang, "Virtual reality and augmented reality combination as a holistic application for heritage preservation in the UNESCO World Heritage Site of Melaka", *International Journal of Social Science and Humanity*, *4*(5), 333, 2014.

[7] V. Venkatesh, M.G. Morris, G.B. Davis, and F.D. Davis, "User acceptance of information technology: Toward a unified view," MIS Quarterly, vol. 27, no. 3, pp. 425-478, 2003.

[8] U. Sekaran, and R. Bougie, "Research Methods for Business. In Research methods for business" pp. 436, 2013.

Development of an optimized thermoelectric cooler for active processor cooling

Z. Abdullah[1*],N. Mokhtar, M.M. Ghazaly[2], M.A.M. Ali[1],K.F. Samat[1], T.A. Abdullah[1], N.S. Muhammad[3]

[1)] Faculty of Manufacturing Engineering, Universiti Teknikal Malaysia Melaka, Hang Tuah Jaya, 76100 Durian Tunggal, Melaka, Malaysia

[2)] Faculty of Electrical Engineering, Universiti Teknikal Malaysia, Hang Tuah Jaya, 76100 Durian Tunggal, Melaka, Malaysia

[3)] Faculty of Mechanical Engineering, Universiti Teknikal Malaysia, Hang Tuah Jaya, 76100 Durian Tunggal, Melaka, Malaysia

[*]Corresponding e-mail: zulkeflee@utem.edu.my

Keywords: Thermoelectric cooler; active processor cooling

ABSTRACT –The rising heat generation of processor has sparked much interest in active cooling solution. Current cooling solution can't effectively cool down a higher end processor. Thermoelectric cooler is one possible solution for this problem, where when voltage is applied it would create a temperature difference between the surfaces. This allows heat exchange to occur at a morerapid rate. However thermoelectric cooler problems arehigh power consumption, high power dissipation, and low coefficient of performance (C.O.P). Thereforethis project aims tooptimize the thermoelectric cooler for active processer cooling. A prototypewas designed, and fabricated and has optimized power consumption.

1. INTRODUCTION

Modernisation has brought the advancement of central processing unit to a higher stage compared to the last few decades. However the advancement of central processing unit also increases the power consumption and releases more heat than their predecessor. Therefore the central processing unit need requires more heat dissipation in the form of CPU cooling solution[1]. Normally the optimum operating temperature of a central processing unit is at room temperature, or ideally as cool as possible. A hot central processing unit would cause problems, ranging from system crashes and physical damages due to overheating. Common CPU failure mechanisms tend to be mechanical (wire bond failure, die fracture, corrosion) and electrical (overstress, migration and diffusion, gate oxide breakdown). Following the Arrhenius equation, (for die temperatures operating in the range of -20ºC to 140ºC) every 10ºC decrease in temperature reduces the failure rate by approximately a factor of 2. We can therefore expect a reduction in chip failure rates with lower operating temperatures[2].

The growth in central processing unit heat generation has sparked attention in active cooling to bring the temperature down. Critical application of central processing unit in servers or a high performance computer requires an advanced cooler mechanism that would bring the temperature down to an optimum level.

Thus, thermoelectric cooler would be needed to assist the cooling down of the central processing unit. However, there are many problems plaguing thermoelectric cooler. They are notoriously known for their high power consumption, high power dissipation, low coefficient of performance (C.O.P) and limitation due to inefficient system used[3]. Thus in this project, the aim is optimizing of the thermoelectric cooler cooling module for active central processing unit cooling.

2. METHODOLOGY: EXPERIMENTAL SETUP & SYSTEM OVERVIEW

In this section, the research setup & procedures during research are discussed. The design of the prototype considers most design requirement at the earlier stage. It was designed by using Solidworks and fabricated by using a CNC Machine. The proof of concept was using the 4 Drift-0.8 TEC module by Kyrotherm. The designed water block features a four inlet/outflow water route.Adjustable water flow plate was integrated into the water block to investigate whether increased water flow affect the thermal dissipation.

Since the normal thermoelectric cooler design approach which involves direct die cooling has limited cooling capability, direct die liquid cooling offers a better solution (Figure 1). The heat is dispersed by the thermoelectric cooler into a traditional water cooling system which consisted of a water block, pump and a radiator. However this solution is limited to the available space that is present in the central processing unit die area.

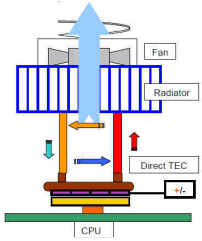

Figure 1 Schematic of direct die liquid cooling [2]

Figure 2 shows the setup for the prototype of the thermoelectric cooler, while Figure 3 shows the bench test done on the prototype.

Figure 2 Setup of the prototype

Figure 3 The bench test

3. RESULTS & DISCUSSION

3.1 Computational Fluid Dynamics (CFD) Analysis

Based on the result, the concept works as intended. Within three minutes the TEC hit a stagnant temperature of -8 Celsius and the trend continue until 15minute passed (Figure 4). Ice formed when it reaches sub-zero temperature (Figure 5). To compare the obtained result with the theory, further calculation was done using the TEC Calculator software. From the TEC calculator, the expected cold side temperature calculated should be at -15.08 Celsius shown in Figure 6. However the result is acceptable since the TEC Calculator doesn't include the thermal resistivity of the cold and hot side of TEC module. Therefore from this result the prototype has shown us great potential.

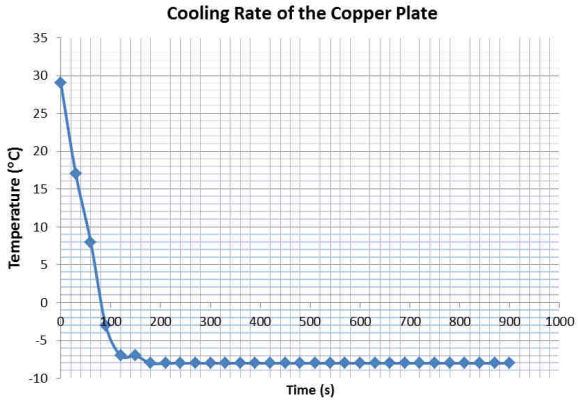

Figure 4 Cooling rate of the copper plate

Figure 5 Ice formed

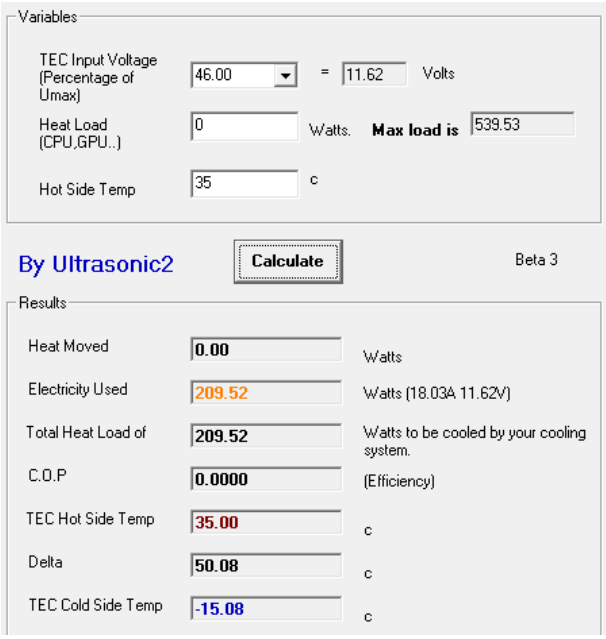

Figure 6 TEC Calculator 46% voltage No-Load

4. CONCLUSIONS

The result shows that the expectation from design concept has been met. However, there are several problems that need to be addressed. The problems are: Some condensation issue, and slight overweight issue causes the motherboard to slightly flex. These problems will be analyzed and solved in the next phase of the project.

REFERENCES

[1] A. Pathak, and V. Goel, (2013). Peltier based Novel Heat Pump for Flow Cell in Automated Analyzer using PWM Techniques.

[2] M. Davis, R. Weymouth, and P. Clarke, "Thermoelectric CPU cooling using high efficiency liquid flow heat exchangers," *International Conferenceon Thermoelectrics*, p. 0–3, 2006.

[3] S. Shaojing and Qinqin, "Temperature control of thermoelectric cooler based on adaptive NN-PID," *Proceedings - International Conference on Electrical and Control Engineering, ICECE 2010*, pp. 2245–2248, 2010.

Reduction of Water Hammer Effect for Domestic Water System

Z. Abdullah[1*], L.W. Wein, M.M. Ghazaly[2], M.A.M. Ali[1], M.S. Kasim[1], R. Jaafar[1]

[1)] Faculty of Manufacturing Engineering, Universiti Teknikal Malaysia Melaka, Hang Tuah Jaya, 76100 Durian Tunggal, Melaka, Malaysia
[2)] Faculty of Electrical Engineering, Universiti Teknikal Malaysia Melaka, Hang Tuah Jaya, 76100 Durian Tunggal, Melaka, Malaysia

[*]Corresponding e-mail: zulkeflee@utem.edu.my

Keywords: Water hammer effect; hydraulic transient; Computational Fluid Dynamics (CFD)

ABSTRACT –Water hammer effect is also known as pressure surge or hydraulic transient, caused by sudden changes of the water distribution network. The water hammer effect can cause serious consequences like pump defects, pipeline failures, bad water quality, and health implications. This research focuses on the design and installation of a surge control device, an accumulator to reduce the water hammer effect. This device stores potential energy in the form of fluid pressure. For the simulation part of the research, 3D CAD drawings of the accumulator was generated and a Motion Simulation Analysis was conducted using the Autodesk (CFD) 2015 software. The best accumulator design is the one with the three bladder balls. The objective of the research is achieved successfully.

1. INTRODUCTION

Water hammer is caused by either planned or sudden changes of the water distribution network. The sudden change in the liquid velocity generates a pressure wave which can have serious effects, ranging from pump defects to pipeline failures[1]. The hydraulic transient phenomenon may also cause bad water quality and health implications. According to a study conducted by Valmatic Valve and Manufacturing Corp (2009) [2], sudden changes in flow speed causes water hammer. In addition, water hammer are caused by pressure in pipelines, speed of water flowing in pipelines and quick change of water speed[3]. Water hammer is highly noticeable while using appliances that require large volume of water, including toilet flushes, washing machines and dishwashers. Accumulators are needed in water systems to absorb the surges and reduce the harmful effects of water hammer[3]. A welldesigned accumulator can reduce and eliminate the results of shock. An accumulator should be installed at or near the point of disturbance, such as the pump discharge or near the closing valve to protect the water system. This setting eliminates hydraulic transient by suppressing pressure pulsations or high pressure surge[2].

2. METHODOLOGY: EXPERIMENTAL SETUP & SYSTEM OVERVIEW

In this section, the research setup & procedures during research are discussed.

SolidWorks CAD drawing was used to generate 3D models of threedifferent designs of the accumulator. Before drawing the 3D CAD model, measurements were taken from the actual prototype product (Figure 1) already created for an experiment to ensure the analysis conducted later in the research would be similar to the experimental data. The designs of each accumulator differ in the number of bladder balls. One, two and three bladder balls were used in each accumulator.

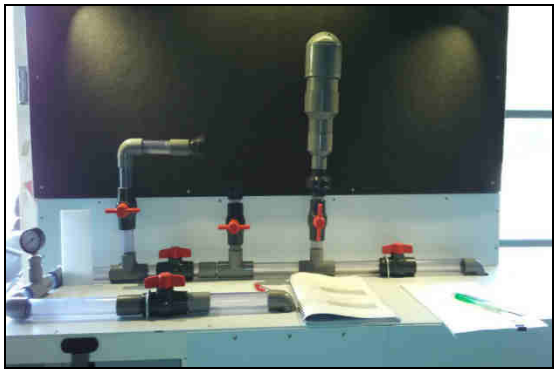

Figure 1 Setup of actual accumulator

3. RESULTS & DISCUSSION

3.1 Computational Fluid Dynamics (CFD) Analysis

A CFD analysis was conducted to analyze the water flow in the accumulator. The purpose of this analysis is to understand the fluid motion in the accumulator and to determine the best design among the three different designs of the portable accumulators. The Autodesk Simulation CFD 2015 software was used during the analysis. The software is able to provide fast, accurate and flexible fluid flow which aids in judging product performance, improve designs and justify product behavior.Table 1shows parameters used in Autodesk Simulation CFD 2015.

After solving the 3D CAD model, several results from the analysis can be displayed including velocity magnitude, static pressure, temperature, density, viscosity and shear stress. The velocity of water flow within the accumulator can be determined either using colour shades or vector magnitude (Figure 2). The following images in Figure 2 shows an example of the accumulator analysis result.

Table 1 Parameters Defined in Autodesk Simulation CFD 2015

Material	Bladder Ball	Silicon Rubber
	Accumulator Body	PVC
Boundary Conditions	Volume Flow Rate (m^3/s)	0.0025
	Pressure (bars)	5
	Temperature (ºC)	25

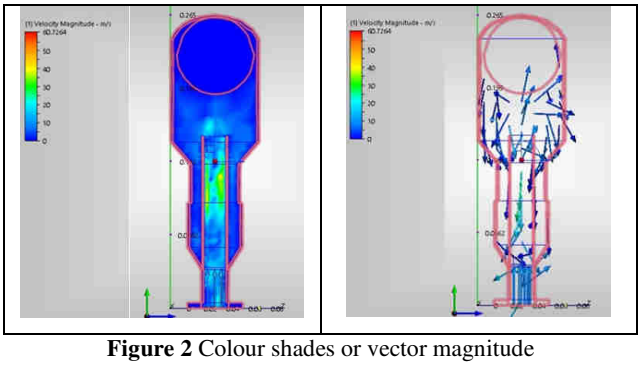

Figure 2 Colour shades or vector magnitude

For the motion flow of bladder balls, when force is exerted, the bladder balls are allowed to move freely within the volume of the cylinder. After defining the parameters, the model is solved and the simulation starts. At the end of the simulation, several results are obtained.In Table2, it is calculated that the accumulator with 3 bladder balls shows the best result, with a water velocity reduction of 81.08%. The reduction of water velocity greatly reduces the occurrence of water hammer. When hydraulic pressure builds up, moving water is displaced by entering the accumulator. Water pressure exerts force by pushing the bladder balls to the maximum end of the accumulator. The momentum of moving water is safely dissipated by reducing the water velocity exiting the accumulator, thus preventing the development of water hammer. For the accumulator with three bladder balls, more volume is available for water displacement. 3 bladder balls are able to absorb the force from the water pressure and acts as a better cushion to reduce the effect of pressure surge. Hence, the water velocity entering and exiting the accumulator is greatly reduced.

Table 2 Comparison for Three Accumulator Designs

Accumulator Design	**Water Velocity (m/s)**		
	In	Out	Percentage Reduction (%)
1 Bladder Ball	46.42	41.63	10.32
2 Bladder Ball	1003.06	689.09	31.30
3 Bladder ball	2007.06	379.84	81.08

From the Table3, it is shown that 5 different materials with different density are compared. Lightweight materials used are ABS, silicon rubber and glass. Materials with higher density used are steel and copper. For copper bladder ball, the percentage velocity reduction is the highest at 67.30% followed by steel at 64.37%. Based on the results from the analysis, it can be concluded that heavy materials such as copper and steel are more suitable to replace silicon rubber material of the bladder ball as they have better properties to reduce the water velocity entering the accumulator. However, model experiments should be conducted to better understand the effects of bladder ball density on the percentage weight reduction and to verify the simulation analysis.

Table 3 Comparison for Bladder Ball Materials

Bladder Ball Material	**Material Density (kg/m^3)**	**Water Velocity (m/s)**		
		In	Out	Percentage Reduction (%)
Silicon Rubber	1700	46.42	41.63	10.32
ABS (Polycarbonate)	1400	17.00	8.06	52.59
Copper	8940	27.40	8.96	67.30
Glass	2700	191.27	108.92	43.05
Steel	7833	177.73	63.33	64.37

4. CONCLUSIONS

A CFD analysis was conducted using the Autodesk Simulation CFD 2015 software to evaluate the performance of three different accumulator designs. The analysis result shows that the best accumulator design to solve the water hammer problem is the accumulator with 3 bladder balls. It is able to reduce the largest percentage of water velocity flowing into the accumulator compared with the other accumulator designs. The reduction of water velocity is important in reducing the impact of water hammer. It acts as a cushion to absorb the pressure surge, hence, water exiting the accumulator have greatly reduced in velocity. While the initial material setup for the bladder ball was silicon rubber, several other materials were also analyzed to obtain the best result for bladder ball material. From the analysis results, it was shown that steel and copper bladder balls, which have higher densities, are able to perform much better than silicon rubber bladder balls. Finally, an analysis was conducted to compare the best bladder ball material for the accumulator design with three bladder balls. Even though steel has a lower density compared to copper, it has better properties which enables the efficiency of the accumulator to be greatly improved. Hence, the best design and material is accumulator design with three steel bladder balls.

REFERENCES

[1] P.F. Boulos, B.W. Karney, D.J. Wood and S. Lingireddy, "Hydraulic Transient Guidelines," *Am. Water Work. Assoc.*, pp. 111–124, 2005.

[2] Valmatic Valve and Manufacturing Corp, "*Surge Control in Pumping Systems*" no. 630, 2009.

[3] T.W. Choon, L.K. Aik, L.E. Aik and T.T. Hin, "Investigation of Water Hammer Effect Through Pipeline System,"*International Journal on Advanced Science Engineering Information Technology*, vol. 2, no. 3, pp. 48–53, 2012.

Proceedings of Innovative Research and Industrial Dialogue'16, pp. 49-50 (May 2017)

Design of PID and nonlinear PID controller for tracking performance of XY table ball screw drive system

R.I.A. Raja Izam*, L. Abdullah, N.H. Zulkifli

Faculty of Manufacturing Engineering, Universiti Teknikal Malaysia Melaka, Hang Tuah Jaya, 76100 Durian Tunggal, Melaka, Malaysia

Corresponding e-mail: izziazrul@gmail.com

Keywords: Nonlinear PID controller; tracking performance; XY table ball screw drive system

ABSTRACT – The objective of this project is to design and validate a PID and NPID for tracking performance of the XY table ball screw driven system and using the MATLAB/Simulink software to validate the controller. The performance of the designed controller was validated numerically and experimentally. The results showed that NPID have better performance than PID in terms of tracking error. RMSE of PID and NPID at *f*=0.5Hz is 0.0601 and 0.0594 respectively. Lower RMSE gives better tracking performance.However, the performance of the controller needs further studies for improvement so it can adapt to various conditions of cutting force disturbance.

1.INTRODUCTION

CNC machine is the basic structure of XY table ball screw drive system. For the machine tool to obtain high accuracy and precise positioning, the presence of disturbance force in the system need to be considered when designing the controller. Disturbance forces are divided into two which are cutting force and friction force. These disturbance forces affect the tracking performance of XY table ball screw drive system. It is impossible to eliminate cutting force disturbance when the cutting tool touches the workpiece. Conventional PID controller has been designed to compensate the cutting force disturbance but it has limitations [1]. To improve the tracking performance in machine tools applications, an efficient and reliable compensation technique is desired in a controller [2]. The design of PID and NPID controller is vital in determining the tracking performance of XY table ball screw drive system. To design a good PID NPID controller, the understanding of control system is important. The requirements of control system analysis and design are to produce a good transient response, minimize the steady-state error and achieving stability [3].

2. METHODOLOGY: EXPERIMENTAL SETUP & SYSTEM OVERVIEW

In this section, the research setup of the project is XY table ball screw drive system which manufactured by Googol Tech. The motor that drives the two axes is coupled with ball screw drive mechanism with a bracket and a sliding rod mechanism to guide it.

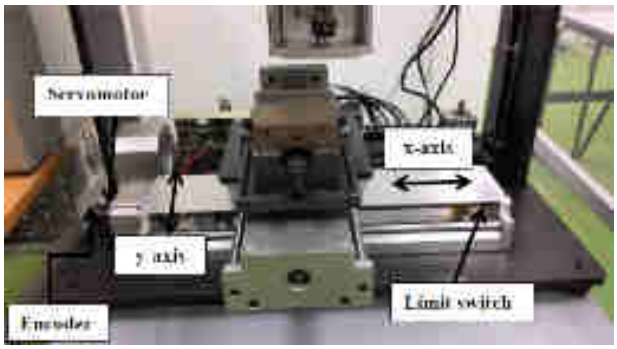

Figure 1 Googol Tech XY Milling Table

Table 1 Main components of the experimental setup

Components	Function
Personal computer with MATLAB / Simulink and ControlDesk	Man-machine interface (MMI) to provide input to the plant and control the motion of both axes.
dSPACE DS 1104 Digital Signal Processing (DSP) board	Provides digital Input/Output (I/O) interfaces for the overall system.
Amplifier	Amplifies the input signal from the host computer to the actuators.
XY table	Use for experimental validation.

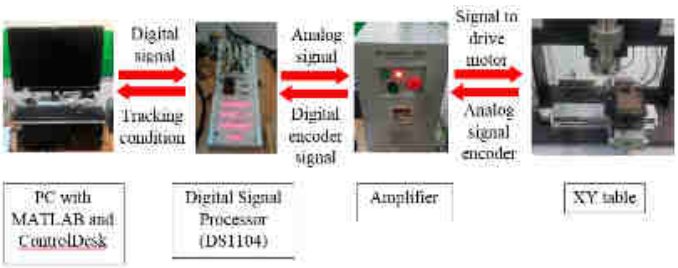

Figure 2 Schematic diagram of the experimental setup

3. RESULTS AND DISCUSSION

Table 2 Simulated and experimental maximum tracking error of the system with PID controller

Frequency (Hz)	Maximum Tracking Error (mm)	Percentage Error (%) [Track * Error / Amplitude] *100%
Simulation		
0.3	0.0492	0.3280
0.5	0.0812	0.5413
Experimental		
0.3	0.0514	0.3426
0.5	0.0861	0.5740

The amplitude used in this research project was 15mm. Thus, the percentage error is calculated for both simulation and experimental. The experimental results show higher maximum tracking error than the simulation for both 0.3Hz and 0.5Hz.

Table 3 Simulated and experimental maximum tracking error of the system with NPID controller

Frequency (Hz)	Maximum Tracking Error (mm)	Percentage Error (%) [Track * Error / Amplitude] *100%
Simulation		
0.3	0.0320	0.2133
0.5	0.0517	0.3447
Experimental		
0.3	0.0510	0.3400
0.5	0.0853	0.5560

Same goes for NPID controller where amplitude of 15mm is used. The experimental results for NPID are the same as PID where the maximum tracking error is higher than the simulation for both 0.3Hz and 0.5Hz.

Table 4 Comparison in RMSE values for different controller

Frequency (Hz)	Root Mean Square Error (mm)		Percentage Error Reduction (%)
	PID	NPID	
0.3	0.0359	0.0358	0.28
0.5	0.0601	0.0594	1.16

RMSE is quantified because it is more accurate on the tracking performance of a controller compared to maximum tracking error for case where the input signal used is a sinusoidal signal. RMSE propose more solid representation of tracking performance of a controller.

Table 5 Comparison in maximum tracking error for different between PID and NPID controller

Frequency (Hz)	Maximum Tracking Error (mm)			
	PID Controller		NPID Controller	
	Simulation	Experimental	Simulation	Experimental
0.3	0.0492	0.0514	0.0320	0.0510
0.5	0.0812	0.0861	0.0517	0.0834

Tracking errors at 0.3Hz were lower than tracking errors at 0.5Hz. This is due to the speed of the response because the controller have more time to response at lower frequency. PID controller presented higher tracking errors than NPID controller. This is because PID controller only can gain the same parameter but NPID controller has the function of nonlinear gain.

4. CONCLUSION

The designs of the controller were analysed and evaluated based on the maximum tracking error and root mean square error (RMSE). Based on the results, NPID controller has better tracking performance compared to PID controller. The frequency and error has directly proportional relationship where higher frequency will lead to higher error and vice versa. The designed controllers were validated successfully via simulation and experimental work and proven in the maximum tracking error and RMSE. The data from this research can benefits to the industry where better control system can be implemented for machine that has the same characteristics as XY table.

REFERENCES

[1] G. Zhao, Y. Zhao, H. Zhang, Z. Sima and L. Zhang, "Research on PositionController of CNC Machine", *Second International Conference on Intelligent Computation Technology and Automation*, pp. 907–910, 2009.

[2] L. Abdullah, Z. Jamaludin, N.A. Rafan, J. Jamaludin and T.H. Chiew, "Assessment on tracking error performance of Cascade P/PI, NPID and N-Cascade controllerfor precise positioning of xy table ballscrewdrive system", *IOP Conference Series: MaterialsScience and Engineering*, *53*, 2013.

[3] Y. Li, K.H. Ang and G.C. Chong, "PID Control System Analysis and Design", IEEE Contr. Syst. Mag. 26 (1), pp.32-41, 2006.

Water absorption study on woven jute reinforced unsaturated polyester composite using warm compression moulding with and without lay-up process

N. Hakimi[1,2] and Z. Mustafa[1*]

[1)] Sustainable Materials for Green Technology Research Group, Advanced Manufacturing Centre, Faculty of Manufacturing Engineering, Universiti Teknikal Malaysia Melaka, Hang Tuah Jaya, 76100 Durian Tunggal, Melaka, Malaysia

[2)] Department of Polymer Composite Processing Technology, Kolej Kemahiran Tinggi MARA, 76400 Masjid Tanah, Melaka, Malaysia

*Corresponding e-mail: zaleha@utem.edu.my

Keywords: Jute fibre; unsaturated polyester; water absorption; warm compression moulding; hand lay up

ABSTRACT – Woven jute fibre reinforced unsaturated polyester composites at 40 vol.% fibre content were fabricated using warm compression moulding at the optimize parameters of 163°C, 4 MPa of pressure and held in the mould for nearly 1069 seconds, with and without additional hand lay-up process. Both composite was immersed in distilled water at 27°C for period of 1,2,3,4,5,6 and 7 weeks to investigate the effect of the water absorption to their mechanical properties. The water absorption found to be lower in composite fabricated with additional of hand lay–up. The flexural properties were found to decrease with the increase in percentage water uptake. This flexural behaviour could contribute from the effect of plasticization that occurred at the matrix–fibre interface resulting in swelling of the jute fibres.

1. INTRODUCTION

Jute as natural fibres are made up of cellulose, hemicelluloses, pectin, lignin, and water mainly. The application of natural fibres to component design through polymers is limited by hydrophilic nature of the cellulose [1-3]. Natural fibres have a few disadvantages when used as reinforcements, such as higher moisture absorption which brings about dimensional changes thus leading to micro-cracking and poor thermal stability [3-5]. As this process mostly occurred at the interface of the composite, better wettability and lower porosity of the composite are expected to influence the water intake. Thus this paper focused on water absorption the study and their effects on the woven jute reinforced unsaturated polyester composite with respect to the variant in the composite fabrication

2. METHODOLOGY

Materials

The jute fibres used are in woven form (Composite Evolution, UK) as reinforcement. The matrix is unsaturated polyester resin (Revertex Sdn. Bhd).

Composite Fabrication

Prior to the fabrication, the jute fibres were pre-treated using 5% NaOH. The jute/ unsaturated polyester composite panel at 40 vol. % fibre content were lay-up in a 300mm x 300mm x 3mm (width, length and thick) mould and the required resin in pour directly on the top of the woven fibres. It was then compressed moulded using hot press (Gotech, Taiwan) at the optimised conditions of 163°C, 4 MPa of pressure and held in the mould for nearly 1069 seconds. To compare the influence of the fabrication parameter, for the second sample, the resin was applied onto each of the ply using hand lay-up method and followed by compression moulding using same parameters. The samples were cut into 100mm x 12mm x 3 mm for further testing.

Water Absorption

The water absorption testing was carried out according ASTM D570. Each of the sample were weighed (W_o) to nearest 0.001g and then immersed in distilled water at a temperature of 27°C at interval week of 1,2,3,4,5,6 and 7 weeks. For water absorption measurement, the sample were withdrawn from the water at each interval week, and wiped with a dry cloth to remove any existing surface water and immediately weighed (W_t). The moisture content (M_T) for each specimen is determined by using Equation 1[6]:

$$M_T = \frac{Wt}{W_o} \times 100\,\% \qquad (1)$$

1.3 Flexural Strength

The flexural properties were characterized using Instron 3385 universal testing machine with cross head speed of 2 mm/min (ASTM D 790). Specimens with the span to depth ratio of 16:1 were used. The flexural strength and using Equation 2:

$$\sigma = 3PL/\ 2bd^2 \qquad (2)$$

Where P is the load, L is the span length of the sample, b is the width, d is the thickness and m is the gradient or the deflection of the curvature.

3. RESULTS AND DISSCUSSION.

3.1 Absorption Behaviour

The percentage of water absorption plotted against immersion time is shown in Figure 1. Each data point indicating the average of five samples. The composite absorb water very rapidly in the initial stage until a saturation point is attained. The prepared composite with additional hand –lay-up process has lower percentage of water intake in comparison to the composite without. This suggesting that water was absorption thru the matrix-fibre interface and pores in the composite. The composites absorb water rapidly at the initial stage until it reaches saturation point (week 4). Afterward, the composite started to degrade resulting in decreased in weight lost. Moreover, a degradation process occurs when the fibres swell due to moisture absorption. Micro gaps are formed between the fibres and resin matrix, which results in the formation of water transport pathways within the composites in which increased the water uptake after the saturation point is achieved [6].

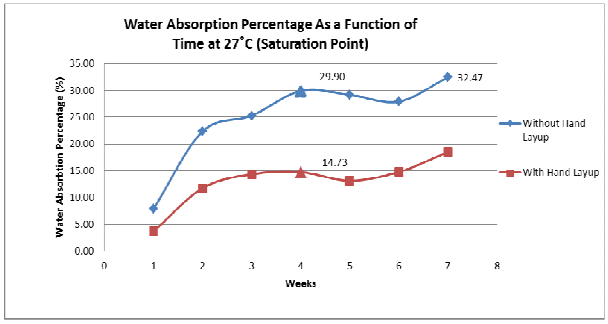

Figure 1 Water Absorption of Jute/Unsaturated Polyester at 27˚C

3.2 Flexural Strength

The effect of the water degradation on the flexural strength of the composite is shown in Figure 2. It can be observed, for both composite, the flexural strength was decreased with increased of immersion time. Decreased in the flexural strength after water immersion is due to formation of hydrogen bonding between the water molecules and cellulose fibre [7].

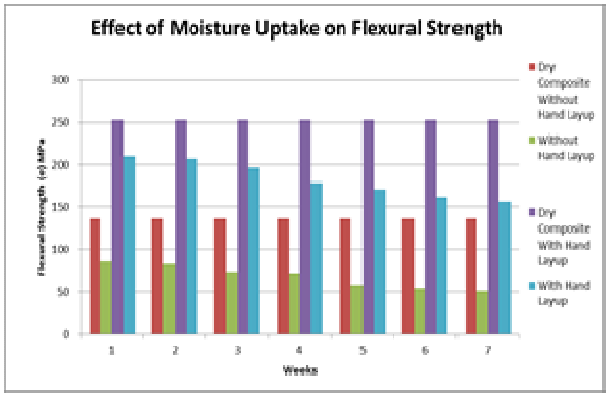

Figure 2 Effect of the water immersion on flexural strength of the composite

4. CONCLUSIONS

The water absorption is lower in composite fabricated by combining hand lay-up and compression moulding. Saturation point was observed at week 4 in which afterward the composite started to degrade. Similar trend was observed in flexural strength. Composite fabricated using hand-lay-up and compression moulding showed higher flexural strength. Both composite showed decreased in flexural strength with increase of immersion time due to due to degradation of the fibre-matrix interface.

ACKNOWLEDGEMENT

Authors are grateful to Majlis Amanah Rakyat (MARA) for the financial support and Universiti Teknikal Malaysia Melaka.

REFERENCES

[1] N. Jauhari, R. Mishra and H. Thakur, "Natural Fibre Reinforced Composite Laminates – A Review," *Materials Today: Proceedings*, vol. 2, no. 4–5, pp. 2868-2877, 2015.

[2] H.M. Akil, "Environmental effects on the mechanical behaviour of pultruded jute/glass fibre-reinforced polyester hybrid composites," *Composites Science and Technology*, vol. 94, pp. 62-70, 2014.

[3] A. Gopinath, M.S. Kumar, and A. Elayaperumal, "Experimental Investigations on Mechanical Properties Of Jute Fiber Reinforced Composites with Polyester and Epoxy Resin Matrices," *Procedia Engineering*, vol. 97, pp. 2052-2063, 2014.

[4] W.Z.W. Zahari, "Mechanical Properties and Water Absorption Behavior of Polypropylene / Ijuk Fiber Composite by Using Silane Treatment," *Procedia Manufacturing*, vol. 2, pp. 573-578, 2015.

[5] Athijayamani, A., et al., "Effect of moisture absorption on the mechanical properties of randomly oriented natural fibers/polyester hybrid composite," *Materials Science and Engineering A*, vol. 517, no. 1–2, pp. 344-353, 2009.

[6] M. Haameem J.A. , M.S. Abdul Majid, M. Afendi, H.F.A. Marzuki, E. Ahmad Hilmi, I. Fahmi, A.G. Gibson, "Effects of water absorption on Napier grass fibre/polyester composites," *Composite Structures*, vol. 144, pp. 138-146, 2016.

[7] M.K. Gupta, and R.K. Srivastava, "Effect of Sisal Fibre Loading on Dynamic Mechanical Analysis and Water Absorption Behaviour of Jute Fibre Epoxy Composite," *Materials Today: Proceedings*, vol. 2, no. 4–5, pp. 2909-2917, 2015

Proceedings of Innovative Research and Industrial Dialogue'16, pp. 53-54 (May 2017)

Identification and control of hand grasping force for upper limb prosthetics system using noninvasive electromyography technique

M.N. Maznan[1], R. Ghazali[1*], C.C. Soon[1], M.H. Jali[1], M.Z.A. Rashid[1]

[1)] Faculty of Electrical Engineering, Universiti Teknikal Malaysia Melaka, Hang Tuah Jaya, 76100 Durian Tunggal, Melaka, Malaysia.

[*]Corresponding e-mail: rozaimi.ghazali@utem.edu.my

Keywords: Hand grasping force; upper limb prosthetics system; noninvasive electromyography technique

ABSTRACT – This study deals with the grasping force control of upper limb prosthetics hand by using noninvasive electromyography (EMG) technique, for the purpose of measurement on the electrical signal occurred during the contraction and relaxation cycles of human forearm muscle. Proportional-integral-derivative (PID) controller is used to track the desired force based on the transfer function of force obtained through the system identification toolbox. Besides that, optimization toolbox is used to improve the force tracking performance. The SolidWorks software is utilized in the development of the hardware parts, while LabVIEW is used for the data collection purposes. The experimental and numerical results indicate the designed prosthetics hand, which is controlled through an optimized PID controller is capable to fairly tracking the desired hand grasping force.

1. INTRODUCTION

Nowadays, cosmetic prosthetics hand has been widely created to replace the human hand that is not capable to accomplish the task normally, which is lost or damaged caused by war, trauma, accident or congenital anomalies. The development of prosthetics hand is necessary to maintain the quality of life for the people who have lost their hand and allowed them to continue their routine activities. A design of prosthetics hand, which is according to the real human hand situation must taking every details into consideration such as force, movement, and functionality at a fingertip, which will able to hold an object and grasp it with an adequate amount of force by using an Electromyography (EMG) instrument.

EMG is used to recognize the pattern from human muscle and convert it into electrical signal, which will later transform into dynamic movement of prosthetics hand. However, it is well known that the pattern recognized by EMG may change according to the different person, who has their own different structure of body muscle such as thickness of fat on forearm, the fatigue and sweat can change the time variant [1].

A rising number of works by engineers and researchers to fabricate and develop a prosthetics hand that is similar to a human hand has been reported in the past several years. The movement of human hand can be replaced by adding some instrument and motor to a prosthetics hand.

The EMG instrument is able to measure the muscle electrical signal and produce a dynamic movement to the motor. A compound and adaptable structure is making the prosthetics hand produce higher grasping power on heavy object, which is achieved by the combination of large number degree of freedom (DOF), proprioceptive, exteroceptive sensor and a complex hierarchical architecture control [2].

However, a survey that was conducted in [3] reported that 30 - 50% of the upper extremity amputees are not using their prosthetics hand frequently. The defect remonstrated by these subjects included limited controllability, poor cosmetic appearance, and reduced functionality. In order to conduct more daily routine activities, these subjects would like to improve the grasping functions capability. Furthermore, subjects also required sensory feedback function to be able to feel their prosthetics hand as a part of their own body.

In this paper, a prosthetics hand has been designed by using SolidWorks software and fabricated by using three Dimension (3D) printer. The design of prosthetics hand will be validated with the noninvasive EMG technique. The designed prosthetics hand is associated with the human hand by using single actuators and muscle sensor, which will provide a dynamic of prosthetics hand through forearm muscles and nervous system.

2. DEVELOPMENT OF PROSTHETICs HAND

The designed prosthetics hand by using SolidWorks software and fabricated through three-dimension (3D) printer is depicted in Figure 1 below.

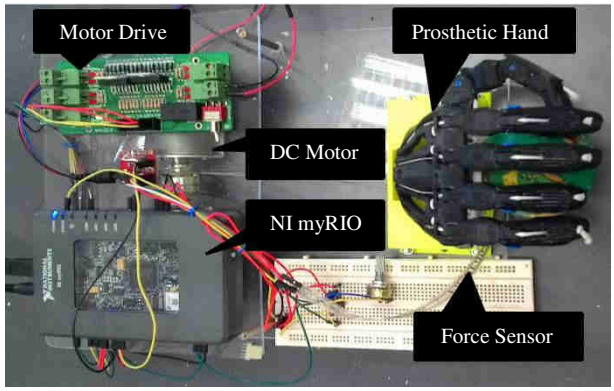

Figure 1 The designed prosthetics hand

To design the prosthetics hand, SolidWorks software was used to draw and assemble all the parts in prosthetics hand followed by the 3D printing process,

which was used to fabricate the designed model. The system was later constructed using LabVIEW software from National Instrument. In the LabVIEW software, visual instrument (VI) panel was used to placing all the needed measurement instrument.

After the establishment of VI panel, the testing on the fabricated prosthetics hand through the hardware circuit to confirm the program is correctly installed is needed. In the LabVIEW software, output data was transferred into MATLAB/Simulink System Identification Toolbox. In addition, an optimization technique was applied in order to obtain better PID controller performance.

3. RESULTS AND DISCUSSION

The force generated from human forearm muscle was measured through EMG instrument and produced an electrical signal, which was converted into the dynamics of the DC motor. The best fit EMG transfer function has been obtained through system identification toolbox as tabulated in Table 1 below.

In Table 1, it is clearly seen that the highest best fit is the transfer function number two with 72.49 percent best fit. The transfer function that has a highest or best percentage will be used to convert the value of EMG electrical signal to the form of torque.

Table 1 The transfer function of EMG instrument

No.	Transfer Function Equation	Best Fit (%)
1.	$\frac{0.007599\,z \quad 0.005521}{z^{2} \quad 1.063\,z \quad 0.3944}$	72.48
2.	$\frac{0.009183\,z \quad 0.006501}{z^{3} \; 2.017\,z^{2} \quad 0.491z \quad 0.4064}$	72.49
3.	$\frac{0.008009\,z^{2} \quad 0.01129\,z \quad 0.00635}{z^{3} \quad 0.1389\,z^{2} \quad 0.5707\,z \quad 0.003582}$	72.46

The response of system identification toolbox that generated the transfer function and best fit percentages is shown in Figure 2 below.

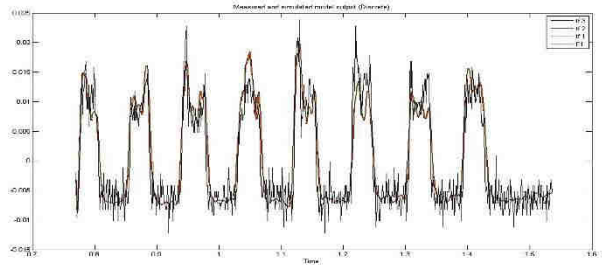

Figure 2 Identification using EMG signals

To obtain the optimal performance of the designed prosthetics hand, the PID controller is applied to increase the force tracking accuracy. Ziegler-Nichols conventional tuning method is first applied to obtain the PID controller parameter, followed by an optimization technique to achieve optimum PID controller parameters. The response of the motor controlled through PID controller was illustrated in Figure 3.

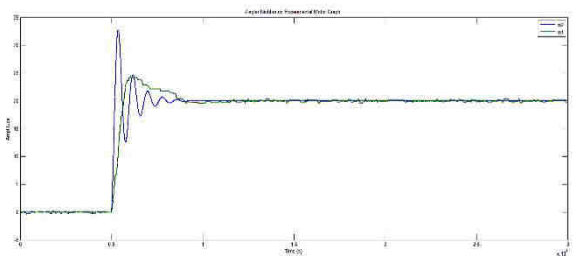

Figure 3 System performance using PID controller

Table 2 below indicates the optimal PID value obtained through MATLAB optimization toolbox.

Table 2 Optimal PID value

PID Controller	Kp	Ki	Kd
Motor 1	2.058	2	0.5

4. CONCLUSION

In this paper, the hand grasping force control of upper limb prosthetics hand by using noninvasive electromyography (EMG) technique for the measurement of electrical signal occurred during the contraction and relaxation cycles of human forearm muscle has been assessed. It is concluded that the transfer function obtained through system identification toolbox playing vital role in the performances of overall system. From the obtained simulation and experimental results, it can be inferred that the motor was able to produce the required torque from the electrical signal generated through the electromyography instrument with the help of PID controller. The fabrication and design development of the prosthetics hand will produce a helping hand for the people with disabilities to continue their routine with an appropriate grasping force.

REFERENCES

[1] C. Castellini and P. van der Smagt, "Surface EMG in advanced hand prosthetics," *Biol. Cybern.*, vol. 100, no. 1, pp. 35–47, 2009.

[2] A. Ninu, S. Dosen, S. Muceli, F. Rattay, H. Dietl and D. Farina, "Closed Loop Control of Grasping with a Myoelectric Hand Prosthesis: Which Are the Relevant Feedback Variables for Force Control?" *IEEE Trans. Neural Syst. Rehabil. Eng.*, vol. 22, no. 5, pp. 1041–1052, 2014.

[3] C. Cipriani, F. Zaccone, S. Micera and M. C. Carrozza, "On the Shared Control of an EMG-Controlled Prosthetic Hand: Analysis of User-Prosthesis Interaction," *IEEE Trans. Robot.*, vol. 24, no. 1, pp. 170–184, 2008.

Surface roughness monitoring during machining HTCS 150 hardened steel under various cutting parameters

A.B. Hadzley[1*], A.A. Anis[1], M.S. Kasim[1], R. Izamshah[1], M.O Hairizal[2]

[1)] Faculty of Manufacturing Engineering, Universiti Teknikal Malaysia Melaka, Hang Tuah Jaya, 76100 Durian Tunggal, Melaka, Malaysia.

[2)]Faculty of Engineering Technology, Universiti Teknikal Malaysia Melaka, Hang Tuah Jaya, 76100 Durian Tunggal, Melaka, Malaysia.
[*]Corresponding e-mail: hadzley@utem.edu.my

Keywords: Machining; HTCS 150 hardened steel; surface roughness

ABSTRACT – This paper presents the preliminary results for HTCS 150 machining using SRFT 20 VP15TF coated carbide ball mill to study parameters effect on surface roughness. Experiments were conducted with limited 10000 passes at variable cutting speeds of 6116 to 14667 rpm, feed rates of 2447 to 7051 mm/min and depths of cut of 0.1 to 0.5 mm using MAZAK Variaxis 5-axis CNC milling machine. From the experiment, the lowest value of the surface roughness is 0.21µm which is recorded for combinations of 14103 rpm, 4231 mm/min and 0.1 mm. On the other hand, the highest value for the surface roughness recorded at 0.926 µm for combinations of 8511 rpm, 4255 mm/min and 0.3 mm. Fine surface roughness being important requirement to determine the final product quality and avoid secondary process for finishing conditions.

1. INTRODUCTION

Hot stamping is a process of creating metal parts by applying high pressure to a part using special made dies and forming the metal into a desired shape. During hot stamping process, a blank part is heated up before stamped in the die enclosure. At this stage the die will provide cooling, assisted by the cooling channel inside the die to quench the heated blank part. For efficient quenching process, the surface roughness of the die should be as fine as possible for better heat transfer during die-to-blank contact [1].

One of the special designed die that applied in hot stamping application is High Thermal Conductivity Steel (HTCS 150). HTCS 150 possess almost similar mechanical properties as SDK 11 (common material used for stamping die) except higher thermal conductivity (up to 66 W/m.K), which is almost triple to provide better cooling [2]. This material is considered new in metal stamping industries. Therefore, the resources of works that presenting the surface roughness characteristics of HTCS 150 is very limited.

This research presents the machining characteristics of HTCS 150 hardened steel materials at various machining parameters. Here, the surface roughness of each HTCS 150 hardened steel material is monitored at different cutting speeds and feed rate. Set of cutting parameters were selected as the preliminary investigations to correlate the combination of these parameters on surface roughness. The understanding and correct use of these parameter not only will lead to a better surface finish that provide efficient quenching process inside the die but also to avoid secondary process for finishing surface conditions of HTCS 150.

2. METHODOLOGY

This experimental work is to evaluate the effect of machining parameter on machined surface roughness during the end milling process. The HTCS 150 hardened steel was used in the experiment. The test specimen is a square block (50 mm by 50 mm) with thickness of 10 mm. This experiment was conducted using MAZAK Variaxis 5-axis CNC milling machine to study the machining surface roughness with respect to the changes in speed, feed rate and depth of cut. The type of insert used in this work was manufactured by Mitsubishi carbide coded as SRFT 20 VP15TF as shown in Fig. 1. For each sample, the machining was held up to 10,000 passes where the surface roughness was monitored at period of 1250 passes. Surface roughness of all specimens was measured after each machining using a portable Mitutoyo SJ-301. Table 1 shows the cutting parameters used in this study.

Figure 1 Insert for ball end mill 20mm

Table 1 Cutting Condition for machining tests

No.	Cutting speed (m/min)	Feed rate (mm/tooth)	Depth of cut (mm)
1	130	0.4	0.1
2	120	0.4	0.5
3	125	0.5	0.1
4	120	0.4	0.1
5	130	0.5	0.3
6	125	0.3	0.1
7	130	0.3	0.3
8	120	0.5	0.3

3. RESULT AND DISCUSSION

Figure 2 shows a graph of surface roughness value and step over of the experiment. From the graph, 1250 to 5000 passes is the early stage and 5000 to 10000 is the second stage. In the first stage, there are no significant differences shown between the experiments while in the second stage there are noticeable changes. The lowest value was found at the experiment 6, recorded at 0.21µm (combinations of 14103 rpm, 4231 mm/min and 0.1 mm) while the highest value from first stage to second stage are obtained in the experiment 5, recorded at 0.926 µm (combinations of 8511 rpm, 4255 mm/min and 0.3 mm). This is suspected due to the likeliness of the cutting tool starting to wear.

Figure 3 shows the average of surface roughness value calculated throughout the 10000 passes monitoring. The highest value of average surface roughness is obtained in experiment 5 which is 0.6347 µm and the lowest value for the average surface roughness is 0.3235 µm in experiment 6. Surface roughness is directly influenced by the tool nose radius shape during tool work piece contact. The shearing action from the cutting tool creates peak and valley gap according to the size of tool nose radius [3]. At the early stage, the edge of cutting tool considered still new and sharp. Low surface roughness might be appeared due to right combination between cutting speed, feed rate and depth of cut where the rotational and overlap movements of cutting tool effectively shear the steel to the lower centre line average. On the other hand, high surface roughness might be due to combination of cutting speed, feed rate and depth of cut that not properly interacted where some shearing process on the steel surfaces experienced inappropriate combination to shear the steel smoothly.

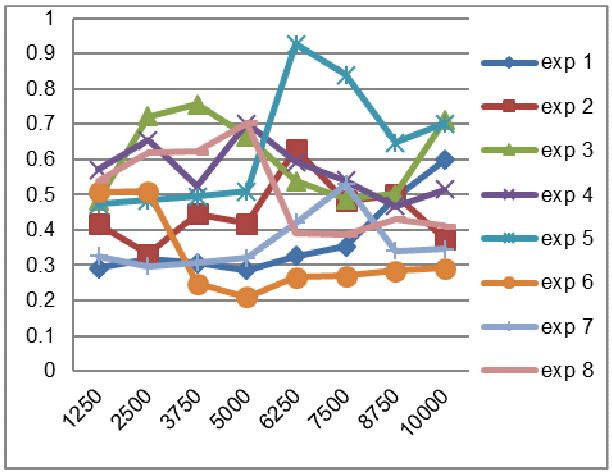

Figure 2 Surface roughness value (Ra) vs step over

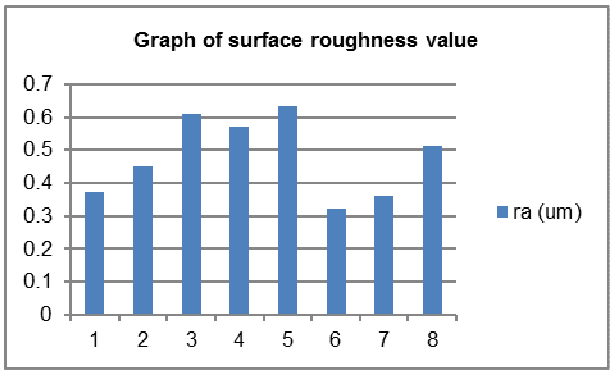

Figure 3 Surface roughness value vs number of experiment

4. CONCLUSIONS

This paper presents the experimental of surface roughness of HTCS 150 hardened steel. From the machining data collected, there are several conclusions can be made.

i. Optimum cutting parameter recorded for lowers surface roughness appeared to be combinations of 14103 rpm, 4231 mm/min and 0.1 mm.
ii. Maximum surface roughness recorded at combinations of 8511 rpm, 4255 mm/min and 0.3 mm.
iii. Proper selection of the cutting parameter for the machining is extremely important factor that need to be considered.

ACKNOWLEDGEMENT

The authors wish to thank the Ministry Of Education Malaysia and Faculty of Manufacturing Engineering, Universiti Teknikal Malaysia Melaka (UTeM) for financial supports through the grant FRGS/2/2013/TK01/FKP/02/1/F00175. The authors also would like to thank Miyazu (M) Sdn. Bhd. for material supplies in this study.

REFERENCES

[1] A.B. Shapiro. Finite Element Modeling of Hot Stamping, *Steel Research International,* vol. 80, pp. 658, 2009.
[2] Rovalma: Manual HTCS-150 state 06/2012.Terrassa (2012).
[3] A.B. Mohd Hadzley, M.N. Farizan, M. O. Hairizal, T. Norfauzi, A. Anis Afuza. Analysis of Surface Integrity and Formatio of Side Flow in Dry and Wet Machining of Aluminum Alloy, in *International Conference on Design and Concurrent Engineering 2016 (IDECON 2016).*

Application of RFID in inspection system in assembly process

M.M. Nor Azhar*, L.Abdullah, N.A.Rosli

[1)] Faculty of Manufacturing Engineering, Universiti Teknikal Malaysia Melaka, Hang Tuah Jaya, 76100 Durian Tunggal, Melaka, Malaysia

*Corresponding e-mail: SergioMuhaimin@gmail.com

Keywords: RFID technology, inspection system

ABSTRACT – "RFID based for Inspection System during Assembly Operation" will explain about an understanding of the application Radio Frequency Identification (RFID) in inspection system during an assembly operation. Methods used in inspection system for tracking and identify the assembly product are by manual, bar code, and vision system. But those methods are still produce an error in inspection. Moreover, manually collecting data require a significant amount of time and labors. RFID is widely used in manufacturing because the applications can reduced cost, increased speed and more accurate. This project will study and analyze the application of RFID into the inspection system.

1. INTRODUCTION

Inspection system is the important process to make sure the product that produced in standard quality and following the line of customer requirement. Effective and efficient quality management based inspection systems are needed to complete the customer order with the standard quality requirement. An automated inspection is the way to get accuracy in inspection process, reduce labour cost, and reduce error. Identification is one of the ways to inspect the correctly part or identify an existing of the part that flow in production process. Automatic Identification and Data Capture (AIDC) are require in identifying process to tracking the part and collect the data automatically. One of the popular identifying technologies is Radio Frequency Identification (RFID). RFID is one of the hottest technologies around and it will impact our lives much more than we realize. RFID technology functioning with a RFID tag or marker can be attached to an individual item giving that product or animal a unique identifier. The number is encrypted within each RFID chip and by using scanning device then activates the particles within the RFID chip to enable it to read the code by using electromagnetic waves. The main obstacle in spreading RFID in manufacturing is the success of barcodes, the previous generation of auto-ID technology. Reading barcodes requires human intervention, a clean, high-contrast environment, and often more than one attempt. Moreover, the amount of data that can be stored in a bar code is much smaller than in an RFID tag, but it cannot be updated. In many applications the functional potential of RFID may not yet beat the low cost of barcodes, but it is only a matter of time before it does.

The emergence of RFID technology into the inspection recording process has simplified and making it easy to understand and implement, and ensures compliance with local standards and regulations.

2. METHODOLOGY

Here, it will discuss about the procedure to achieve the project objectives. There are several method and procedure that will be use. The flow chart is constructed as a guide to make sure the procedure of research is on the track. The detail schedule of research activities are presented in the planning Gantt chart. This project with the title "RFID Technology based Inspection System during Assembly Operation" will be overview about the application of RFID in inspection system during the assembly process in manufacturing sector [1]. From the title given, the problem statements are defined. The problem of this title is about the failure or error in the current inspection system. The next stage of this project is studying all of the literature reviews that have been search from the book, journals, and internet. The understanding of this project is very important before begin the work. An appropriate procedure is chosen to make sure an analysis is acceptable. Design is involved by sketching the system by hand. Then the more view of the system is integrated into the SolidWorks 2005 Software [2,3]. Next to prove the simulation result analysis, the prototype is developed to test the system in practical. The RFID component is defined such as tags, reader, software, computer. Software interface is developing by using the Visual Basic 6.0 Software. Visual Basic 6.0 is a tool that allows you to develop Windows (Graphic User Interface (GUI) applications. Programs are written to solve problems or perform tasks on a computer. Next, a prototype has been builds in order to perform a test. To ensure the product develops is workable; a few reliability testing will be conducted for developing the prototype [3].

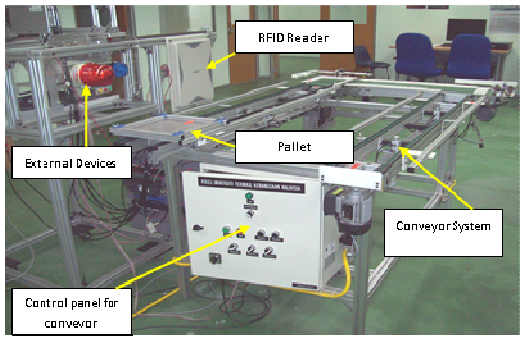

Figure 1 The prototype of inspection system

3. RESULT AND DISCUSSION

The procedures of analysis is measuring the maximum read range of the antenna by reduce the distance between tag and antenna until the reader print the data of tag. When the data of tag is writing by referring to the software interface, that mean the reader can read in that distance which it is the maximum distance. The fifteen of distance is collect by and record in the Figure 2 and construct in the graph as in Figure 3. The analysis is also done in measuring the maximum read distance for left/right side and top/down of the reader. Environmental considerations of an RFID system implementation include the spectrum analysis and the surrounding where the read points are needed. For instance, the RF engineer should consider if tags are required to operate around the liquid or metal. Because different environments tend to have different effects on the RF of the system, it is required that each read point is locally tuned even if the facility where the read point is installed is similar to a prior installation. Tag form factors and inlay selection are important components for this aspect. An analysis is beginning by using the all four products assembly that used different types of material. The tags are attached to each types of material that are archelic, aluminum, mild steel, and stainless steel. The data of reading situation is recorded in Figure 4.

No.	Range to read, (mm)
1	390
2	370
3	380
4	360
5	380
6	370
7	380
8	380
9	390
10	390
11	390
12	390
13	370
14	380
15	370
Average	379.3333333

Figure 2 Middle read range of the Reader

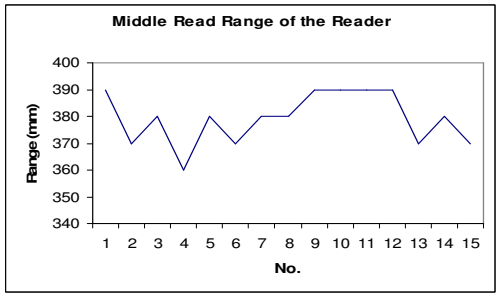

Figure 3 Graph for middle read range of the Reader

Figure 4 The success in reading data due to the types of material

Material of Item	The Success in Reading Data (No.)				
	1	2	3	4	5
Stainless Steel	NO	NO	NO	NO	NO
Mild Steel	NO	NO	NO	NO	NO
Aluminum	NO	NO	NO	NO	NO
Archelic (Part 1)	YES	YES	YES	YES	YES
Archelic (Part 2)	YES	YES	YES	YES	YES

4. CONCLUSIONS

RFID based for Inspection System especially for assembly operation is very interesting and challenging project. In order to make it become successful, a lot of energy, times and money need to be sacrificed. Nevertheless, this project still exposes and enhances the good knowledge for students especially in conducting a research and development of project. Throughout completing this project, there are several keys of developing an inspection system based on RFID. Three main aspects should be considered during design and development of RFID inspection system. There are mechanical structures, electrical circuit and Visual Basic programming.

REFERENCES

[1] L. Zhekun, R. Gadh, and B.S. Prabhu, "Applications of RFID technology and smart parts in manufacturing," In *International Design Engineering Technical Conferences American Society of Mechanical Engineers 2004*, pp. 123-129, 2004

[2] C.K. Haley, C.A. Jacobsen and S. Robkin. *Radio frequency identification handbook for librarians*. Libraries Unlimited, 2007.

[3] D.T. Pham, and R. J. Alcock. *Smart inspection systems: Techniques and applications of intelligent vision*. Elsevier, 2002.

Optimization of process parameters on warpage of plastic part fabricated using injection moulding via Taguchi method

M.A.M. Ali[1,*], N. Idayu[1]

[1)] Faculty of Manufacturing Engineering, Universiti Teknikal Malaysia Melaka, Hang Tuah Jaya, 76100 Durian Tunggal, Melaka, Malaysia

[*]Corresponding e-mail: mohdamran@utem.edu.my

Keywords: Optimisation; warpage; Taguchi method

ABSTRACT – In this study, the main objective is to optimize the injection moulding process parameters such as mould temperature, melt temperature, injection time and cooling time on warpage of plastic. Autodesk Simulation Moldflow software was used to run the simulation of the plastic part to get the recommended parameters. The experiment was conducted by using Taguchi L9 orthogonal array. It was found that optimum parametric combination are at mould temperature of 56 ^{o}C, melt temperatureof 250 ^{o}C, injection time of 0.70s and cooling time of15.4 seconds. The melt temperature was identified as the most significant parameter that affect the warpage of plastic part.

1. INTRODUCTION

Injection moulding is a process to convert thermoplastic material into products by using injection moulding machine. It is reported that material properties, machine parameters and process variables influenced the quality of products [1]. The effect of process parameters on warpage was studied by using Taguchi method as optimization method. It is found that warpage of plastic part was minimized by using optimum combination of processing parameters from the Taguchi approach [2–4].

The objective of this study is to optimize the process parameters such as mould temperature, melt temperature, injection time and cooling time on warpage of part by using Taguchi method.

2. METHODOLOGY

In this study, Taguchi method with total 9 runs with four factors and three level design matrice was used. Mould temperature, melt temperature, injection time and cooling time were considered as the process parameters. The dumbbell shape of plastic part was drawn by using CATIA V5 and the dimension was following the actual mould dimension. Autodesk Moldflow Simulation software was used to achieve the recommended parameter for the part as shown in Figure 1. Material used in this study was polypropylene (PP).

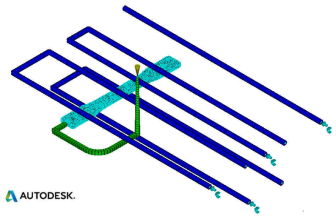

Figure 1 Plastic part in simulation environment

2.1 Parameters of injection moulding process

From the simulation, the software has recommended the parameters at mould temperature (MoT) of 56 ^{o}C, melt temperature (MeT) of 280 ^{o}C and injection time (IT) of 0.7s. The recommended cooling time (CT) of 14 seconds also was obtained from the simulation. According to Wang et al. [5], determination for low level and high level was made by minus and plus 10% of medium value. Therefore, the recommended parameters are set as middle level. Table 1 shows the process parameters setting for the experiment. In addition, the injection moulding used for the experiment was Allrounder 370 H 600-170 Hybrid machine (ARBURG).

Table 1 Process parameters of the experiment

Process Parameters	Level		
	Low	Medium	High
MoT (^{o}C)	50	56	62
MeT (^{o}C)	250	280	310
IT(s)	0.63	0.70	0.77
CT(s)	12.6	14.0	15.4

2.2 Measurement of warpage

The Profile Projector Horizontal (PH-3500) was used to measure the warpage of part. The lenses were focused on the part and the reading of the warpage was displayed by the data board with three decimal places. The measurement of warpage is shown in Figure 2.

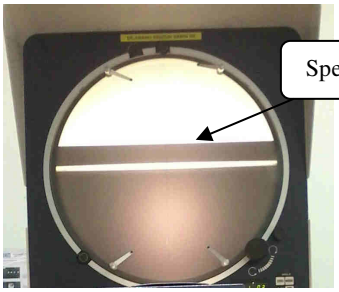

Figure 2 Warpage measurement of plastic part

3. RESULT AND DISCUSSION

3.1 Taguchi analysis

Table 2 shows the warpage result from 9 experimental runs with S/N ratio. The S/N ratio in Taguchi method measures the quality characteristic and the sensitivity of a parameter to uncontrollable factors in the experiment. A greater S/N ratio shows better quality characteristics. The objective is to minimize the warpage.

Table 2 Warpage from Taguchi L9 orthogonal array and S/N ratio

Run	MoT (°C)	MeT (°C)	IT (s)	CT (s)	Warpage (mm)	S/N ratio
1	50	250	0.63	12.6	0.313	10.0891
2	50	280	0.70	14.0	0.299	10.4866
3	50	310	0.77	15.4	0.229	12.8033
4	56	250	0.70	15.4	0.087	21.2096
5	56	280	0.77	12.6	0.378	8.4502
6	56	310	0.63	14.0	0.190	14.4249
7	62	250	0.77	14.0	0.286	10.8727
8	62	280	0.63	15.4	0.339	9.3960
9	62	310	0.70	12.6	0.274	11.2450

3.2 The optimum parameters levels based on S/N ratio

From the S/N ratio graph (Figure 3) and response table (Table 3), it is found that melt temperature is the most significant parameter that affected the warpage of plastic part followed by cooling time, mould temperature and injection time. The S/N ratio graph and value of S/N response table is shown in Figure 3 and Table 3 respectively.

From the graph, it is concluded that the optimum parametric combination are mould temperature of 56°C (Level 2), melt temperature of 250°C (Level 1), injection time of 0.70s (Level 2) and cooling time of 15.4s (Level 3). The optimum parametric combination is the same as run 4. Therefore, run 4 in the experiment is selected as the optimum parameters for minimizing warpage of part.

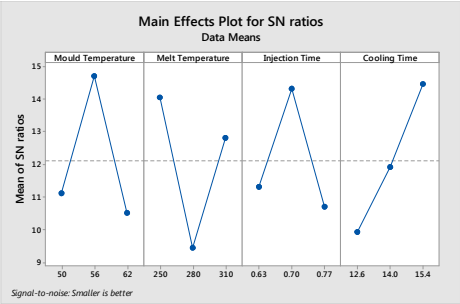

Figure 3 Signal to noise (S/N) graph of warpage

Table 3 Response table for S/N ratio

Level	MoT(°C)	MeT(°C)	IT(s)	CT(s)
1	11.126	14.057	11.303	9.928
2	14.695	9.444	14.314	11.928
3	10.505	12.824	10.709	14.470
Delta	4.190	4.613	3.605	4.542
Rank	3	1	4	2

4. CONCLUSIONS

In this paper, optimization of warpage was studied. It was found that the optimum parameters is the same as run 4. In addition, by using Taguchi method the most significant parameter that affects the warpage is melt temperature, followed by cooling time, mould temperature and injection time.

ACKNOWLEDGEMENT

The authors would like to thank the Universiti Teknikal Malaysia Melaka for providing facilities for this research to be conducted successfully. This research is funded by the Ministry of Higher Education through Research Acculturation Grant Scheme RAGS/1/2014/TK01/FKP/B00075.

REFERENCES

[1] Y.Yang, B.Yang, S.Zhu, and X.Chen, "Online quality optimisation of the injection molding process via digital image processing and model-free optimisation," *J. Mater. Process. Technol.*, vol. 226, pp. 85–98, 2015.

[2] G.Zheng, W.Guo, Q.Wang, and X.Guo, "Influence of processing parameters on warpage according to the Taguchi experiment," *J. Mech. Sci. Technol.*, vol. 29, no. 10, pp. 4153–4158, 2015.

[3] X.Wang, G.Zhao, and G.Wang, "Research on the reduction of sink mark and warpage of the molded part in rapid heat cycle molding process," *Mater. Des.*, vol. 47, pp. 779–792, 2013.

[4] E.Hakimian and A.B.Sulong, "Analysis of warpage and shrinkage properties of injection-molded micro gears polymer composites using numerical simulations assisted by the Taguchi method," *Mater. Des.*, vol. 42, pp. 62–71, 2012.

[5] Y.Wang, J.Kim, and J.Song, "Optimisation of plastic injection molding process parameters for manufacturing a brake booster valve body," *Mater. Des.*, vol. 56, pp. 313–317, 2014.